An investigation of the optical properties of disordered silicon nanowire mats

Hua Bao,[1,2] Weixia Zhang,[3] Liangliang Chen,[2] Haoxiang Huang,[2] Chen Yang,[3] and Xiulin Ruan[2,a)]

[1]*University of Michigan-Shanghai Jiao Tong University Joint Institute, Shanghai Jiao Tong University, Shanghai 200240, China*

[2]*School of Mechanical Engineering and Birck Nanotechnology Center, Purdue University, West Lafayette, Indiana 47907, USA*

[3]*Department of Chemistry, Purdue University, West Lafayette, Indiana 47907, USA*

(Received 18 April 2012; accepted 10 November 2012; published online 17 December 2012)

Optical reflectance spectra of three disordered silicon nanowire mats with average diameters of 40, 60, and 80 nm are investigated both experimentally and theoretically. The total hemispherical reflectance spectra from 200 to 1600 nm wavelength are first measured. All three samples exhibit reflectance about 15% to 20% within the ultraviolet band. As the wavelength becomes longer, the reflectance will first increase to around 50% and then decrease to below 20%. Such reflectance spectra are attributed to the combined effect of silicon dielectric function, the nanowire geometry, and the volume fraction of the mats. An analytical method based on Mie scattering theory and two-flux model is proposed to predict the reflectance spectra of the NW mats using only the physical quantities including dielectric function and structural parameters of the nanowire mats. The experimental reflectance spectra can be well reproduced by this method. © *2012 American Institute of Physics*. [http://dx.doi.org/10.1063/1.4768913]

I. INTRODUCTION

Silicon nanowire (NW) has recently received considerable attention, due to its interesting optical properties and the potential applications for photovoltaics,[1–4] nano antenna,[5] and photo detectors,[6] etc. Recent investigations of the optical properties of silicon NW can be categorized into three different types, including the study of an individual NW, vertically aligned NW arrays, and disordered NW mats. For an individual NW, Cao *et al*. have experimentally demonstrated its frequency-selective optical absorption and scattering properties, which show a quantitative agreement with the prediction of Mie scattering theory.[5,6] For vertically aligned silicon NW arrays, the theoretical works generally employ full-wave numerical electromagnetic simulations,[2,7] and it has been shown that the arrays have extremely low reflectivity. The reflectance measurements confirm such simulation results.[8] Disordered NWs, in contrast, have received less attention. We have previously applied finite-different time-domain simulations to examine the optical properties of aligned NWs with random NW position, diameter, and length.[4] It has been shown that the "partial randomness" can enhance the optical absorption. The completely disordered NW mats with random orientations, however, are too complicated to be investigated by such simulations.

Experimental studies reveal that completely disordered NW mats have much larger reflectance than vertically aligned NWs. But the spectral features of the optical reflectance are quite different, depending on how the NW mats are fabricated. For example, Convertino *et al*. have experimentally studied the optical reflectance of NW mats which are grown using Au films as the catalyst.[9] Their NWs are tapered, which have a thicker bottom and thinner tip. Depending on the average length and diameters of NWs in a sample, the reflectance spectra either show an oscillation with respect to wavelength or show a single maximum.[9] The features in these reflectance spectra are attributed to the optical scattering and the Fabri-Perot effect. Streets *et al*. measured the total reflectance of the two NW mats samples which contain NWs with different diameters from 50 to 200 nm.[10] Their NW mats have a yellow or brown color and each shows a single reflection maximum within 600–800 nm wavelength range. They explained such a curve shape by the different optical characteristics in different spectral regimes, including strong absorption in the short wavelength regime, medium absorption and strong scattering regime in the middle, and low absorption and significant transmission in the long wavelength regime. The different maxima locations in different samples are explained by different contributions of the three effects. An analytical model was also provided.[10] However, the model has too many fitting parameters and the physics is only partly clear. Recently, Brönstrup *et al*. proposed a statistical model based on random-walk approach and Mie-scattering theory which can fit the experimental optical property in the visible range with only three fitting parameters.[11] Actually, the reflectance spectra of silicon NW mats are the complicated results of many factors, including the dielectric property of silicon, NW diameter and distribution, and volume fraction, etc. It is highly desirable to develop a unified predictive model that only uses these physical quantities to calculate optical properties of disordered NW mats.

In this work, the investigations of the total reflectance of disordered silicon NW mats are performed both

a)Author to whom correspondence should be addressed. Electronic mail: ruan@purdue.edu.

experimentally and theoretically. Three samples with different average diameters are fabricated and their optical reflectance spectra are measured. Also, a model based on radiative transport equation (RTE) and Mie scattering theory is proposed to predict the optical reflectance of disordered silicon NW mats. The theoretical and experimental results are compared and discussed.

II. EXPERIMENTAL DETAILS

Silicon NW mats are synthesized by the chemical vapor deposition method with silane as the precursor. Au nanoparticles with uniform diameters are deposited on Al_2O_3/Si substrates as catalyst. The growth is performed with 10 sccm of SiH_4 (10% in H_2) and 40 sccm H_2 at a total pressure of 100 Torr at 460 °C for 10 min. This method allows a quite precise control of the NW diameter and generates NW mats with random orientation and nearly uniform diameter.[12] In one batch, we fabricate three samples with average diameters of 40, 60, and 80 nm, respectively. The SEM images of the 80 nm sample are shown in Fig. 1. Clearly the NWs are not tapered and all NWs in the sample have similar diameters. The thickness of the mat is within the range of 10–20 μm, depending on the location we examined. The 40 and 60 nm NW mats are similar and thus not shown here. To investigate the optical property of the samples, the total hemispherical reflectance spectra of the NW mats are measured by a PerkinElmer Lambda 950 spectrometer with a spectralon coated integrating sphere.

III. MODEL

Unlike the highly ordered structures,[4,13,14] the disordered NW mats with random orientations are too complicated to be studied by full-wave electromagnetic simulations. The investigation of completely random materials is more difficult. The transport theory is often used to obtain an understanding of the light propagation in random media.[15,16] The theory starts by solving the rigorous Maxwell's equations to obtain the scattering and absorption cross sections (σ_s and σ_a) of individual particles. The cross sections characterize the amount of light that is scattered (for σ_s) or absorbed (for σ_a) by the particle. These quantities can then be used as input parameters in RTE. RTE is equivalent to the Boltzmann transport equation, which describes transport of energy through a medium containing particles. The transport theory has been very successful to describe light transport in random media, such as the optical fiber oximeter of blood,[15] polytetrafluoroethylene films,[16] and fibrous materials.[17] Here, the transport theory approach is followed: the NWs are treated as infinitely long circular cylinders with certain diameters and a dielectric function, and the scattering and absorption cross sections are calculated; RTE is then approximately solved to obtain the optical properties of NW mats.

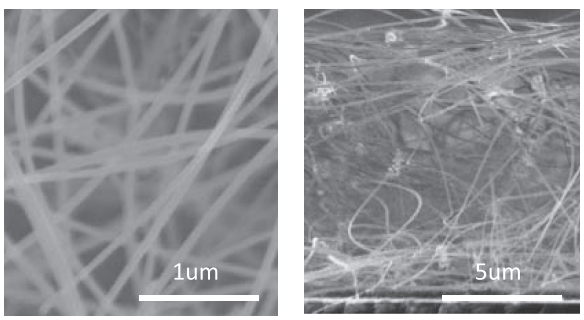

(a) (b)

FIG. 1. The SEM images of the NW mats with 80 nm diameter, (a) top view and (b) side view.

For an infinitely long circular cylinder, the calculation of scattering and absorption cross sections is based on the Mie scattering theory, which is described in textbooks.[18] Simply speaking, one needs to expand the incident and scattered waves into vector cylindrical harmonics and find the expansion coefficients that match the boundary conditions. The expansion coefficients of the scattered wave are a_{nI}, b_{nI} and a_{nII}, b_{nII}, where I and II denote the light polarization parallel and perpendicular to the cylinder axis, respectively. For unpolarized incident light, the scattering and extinction efficiencies (Q_s and Q_e) can be written in terms of these expansion coefficients

$$Q_s = \frac{4D}{k_0}\left[\frac{1}{2}(|b_{0I}|^2 + |a_{0II}|^2) + \sum_{n=1}^{\infty}(|b_{nI}|^2 + |a_{nII}|^2 + 2|a_{nI}|^2)\right], \tag{1}$$

$$Q_e = \frac{2D}{k_0}\mathbf{Re}\sum_{n=-\infty}^{\infty}(b_{nI} + a_{nII}), \tag{2}$$

where D is the diameter of the cylinder and k_0 is the wave vector of the incident light. The absorption efficiency is then calculated by $Q_a = Q_e - Q_s$. These equations have been applied to calculate the scattering and absorption efficiencies for individual silicon NWs, and the results are fairly accurate compared with experiments.[5] The scattering and absorption cross sections per unit length of the infinite cylinder can be calculated from the scattering efficiencies,

$$\sigma_i = Q_i D, \tag{3}$$

where $i = s$ or a (denotes scattering or absorption). They are functions of wavelength λ, NW diameter D, incident angle θ, and dielectric function of the cylinder and surrounding medium.

For random NW mats, it is difficult to investigate the incident and scattering angle of each scattering event, so proper angular averaging needs to be performed. Here, it is assumed that the NWs are randomly oriented in space, and the effective scattering and absorption cross sections can be calculated by averaging all the possible incident angles, i.e.,

$$\sigma_i^{avg}(\lambda, D) = \int_0^{\frac{\pi}{2}} \sigma_i(\lambda, D, \theta)\sin\theta\, d\theta, \tag{4}$$

where $i = s$ or a. Note that a similar equation was used in Ref. 11 to obtain angular averaged cross section. However, the authors failed to include the weighting factor $\sin\theta$, which is the probability of finding a NW oriented at the zenith angle θ.

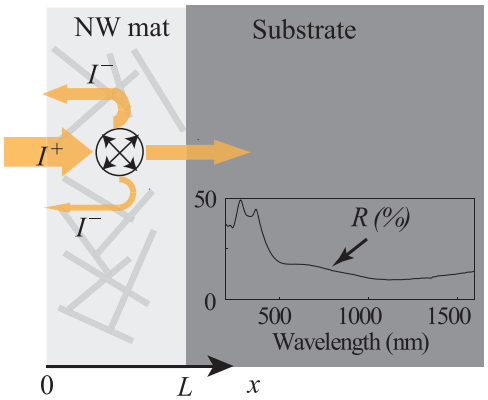

FIG. 2. A sketch of the plane-parallel problem. Inset: the total reflectance of the substrate in air.

To obtain the optical properties of NW mats, we further consider a plane-parallel problem, as shown in Fig. 2. The random NW mat is modeled by a medium with thickness L, which contains many isotropic scatterers with the effective scattering and absorption cross sections as in Eq. (4). The volume average scattering and absorption coefficients of the medium are defined as

$$\langle \sigma_i \rangle = N_s \sigma_i^{avg}, \tag{5}$$

where $i = s$ or a and N_s is the number of scatterers per unit volume. The RTE for such a plane-parallel problem can be approximated solved by the two-flux model, which divides the radiation into forward I^+ and backward I^- components. For non-emitting medium with isotropic scatterers, the following equations have been established:[19,20]

$$\frac{dI^+}{dx} = -(\bar{\sigma}_s + \bar{\sigma}_a) I^+ + \bar{\sigma}_s I^-, \tag{6}$$

$$-\frac{dI^-}{dx} = -(\bar{\sigma}_s + \bar{\sigma}_a) I^- + \bar{\sigma}_s I^+, \tag{7}$$

where $\bar{\sigma}_s = 2B\langle \sigma_s \rangle$ and $\bar{\sigma}_a = 2\langle \sigma_a \rangle$. Here B is the back scattering factor which depends on the angular distribution of the scattered wave. For isotropic scattering, $B = 1/2$, i.e., half of the scattered wave propagates backward. These two equations can be solved analytically given appropriate boundary conditions. At the frontal surface ($x = 0$), it can be assumed that the incident light has unit intensity, so the boundary condition is

$$I^+(0) = 1. \tag{8}$$

At the rear boundary, the boundary condition is related to the optical properties of the substrate. In two-flux model, the effect of the substrate is included by given the boundary condition at the back substrate,

$$I^-(L) = R'_{sub} I^+(L). \tag{9}$$

where R'_{sub} is the reflectance at the NW mats and substrate interface. Note that this is different from the reflectance of the substrate in air R_{sub}. Because the light propagation at the NW-substrate interface is quite complicated, R'_{sub} cannot be directly obtained from experiments or theoretical predictions. Here, we estimate the value from the measurable quantity R_{sub}, which is shown in the inset of Fig. 2. The substrate is an alumina coated silicon wafer, and R_{sub} is less than 20% from 500 to 1600 nm. R'_{sub} should be even smaller because the dielectric contrast at the mat-substrate interface is smaller than air-substrate interface. For wavelength shorter than 500 nm, because silicon is quite absorptive in this wavelength region, it can be expected that only a small amount of light can penetrate the NW mats and interact with the substrate. Therefore, it is reasonable to assumed that there is no back propagating light at the rear boundary, which gives

$$R'_{sub} = 0. \tag{10}$$

For the given boundary condition, the solution of Eqs. (6) and (7) is

$$I^+(x) = \frac{(1+\beta^2)\sinh[\gamma(L-x)] + 2\beta\cosh[\gamma(L-x)]}{(1+\beta^2)\sinh(\gamma L) + 2\beta\cosh(\gamma L)}, \tag{11}$$

$$I^-(x) = \frac{(1-\beta^2)\sinh[\gamma(L-x)]}{(1+\beta^2)\sinh(\gamma L) + 2\beta\cosh(\gamma L)}, \tag{12}$$

where

$$\beta = [\langle \sigma_a \rangle / (\langle \sigma_a \rangle + 2\langle \sigma_s \rangle)]^{\frac{1}{2}}, \tag{13}$$

$$\gamma = [\langle \sigma_a \rangle (\langle \sigma_a \rangle + 2\langle \sigma_s \rangle)]^{\frac{1}{2}}. \tag{14}$$

If we define

$$\beta' = [\sigma_a^{avg} / (\sigma_a^{avg} + 2\sigma_s^{avg})]^{\frac{1}{2}} = \beta, \tag{15}$$

$$\gamma' = [\sigma_a^{avg} (\sigma_a^{avg} + 2\sigma_s^{avg})]^{\frac{1}{2}} = \gamma/(2N_s), \tag{16}$$

the reflectance of the NW mats can be written as,

$$R = I^-(0) = \frac{(1-\beta'^2)\sinh(2\gamma' N_s L)}{(1+\beta'^2)\sinh(2\gamma' N_s L) + 2\beta'\cosh(2\gamma' N_s L)}, \tag{17}$$

where β' and γ' can be determined from Eqs. (15) and (16). If $N_s L$ is known, the total reflectance of the silicon NW mats can be calculated.

IV. RESULTS AND DISCUSSION

A. Scattering and absorption cross sections

Adopting the dielectric function of silicon suggested by Palik,[21] the scattering efficiency Q_s and absorption efficiency Q_a can be calculated. To illustrate the dependence on incident angle, the Q_s and Q_a of an individual 80 nm silicon NW with different incident angles are shown in Fig. 3. It can be clearly seen that the scattering efficiency has quite strong dependence on the incident angle. The absorption efficiency, in contrast, has relatively small angular dependence. These results are consistent with the experimental observations by Cao *et al.*[5] The absorption efficiency for wavelength longer

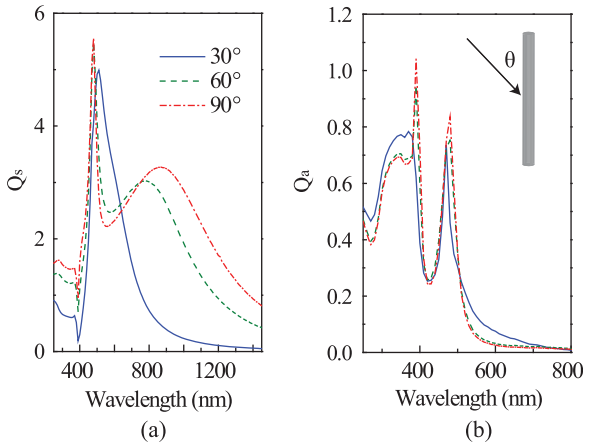

FIG. 3. The (a) scattering and (b) absorption efficiencies of an individual NW with 80 nm diameter at different incident angles.

than 800 nm is nearly zero and thus not shown here. This is due to the small absorption coefficient of silicon in this wavelength regime.

The average scattering and absorption efficiencies of NWs with different diameters are calculated using Eq. (4) and shown in Fig. 4. The scattering and absorption peaks in NWs are due to the leaky mode resonance (LMR) in individual circular cylinders. LMR can be viewed as the effect of multiple total internal reflections within the dielectric cylinder, which occurs when $p(\lambda/n) \approx \pi D$,[22] where p is a positive integer and n is the refractive index of the dielectric material. If a LMR is excited, the NW will respond strongly to the external field. Either a scattering peak or an absorption peak can be observed at such wavelengths. For example, a rough estimation using $n \approx 3.5$ for silicon yields that the lowest order LMR ($p = 1$) occurs at 450 nm for 40 nm NW, which is corresponding to the scattering efficiency peak located at 470 nm. For a NW with 60 or 80 nm diameter, the lowest order LMR occurs at longer wavelength because of the larger NW diameter. From Fig. 4(a), the 60 nm NW has a scattering peak at 600 nm and the 80 nm NW has a peak at 720 nm. There are also other scattering peaks at shorter wavelengths for 60 and 80 nm NWs due to the higher order LMR. In the long wavelength region where the lowest order LMR cannot be supported, the scattering approaches Rayleigh scattering limit. For rods, the theory predicts a λ^{-3} wavelength dependence of scattering,[23] which explains the decaying tail of scattering efficiency in Fig. 4(a). Figure 4(b) shows the average absorption efficiency for NWs with different diameters. Such absorption behaviors of NWs are a combined effect of the absorption coefficient of silicon and the geometry of the NWs. For example, the small absorption efficiency in long wavelength regime can be attributed to the small absorption coefficient of silicon, while the absorption peaks can either be attributed to the LMR or the large absorption of silicon.

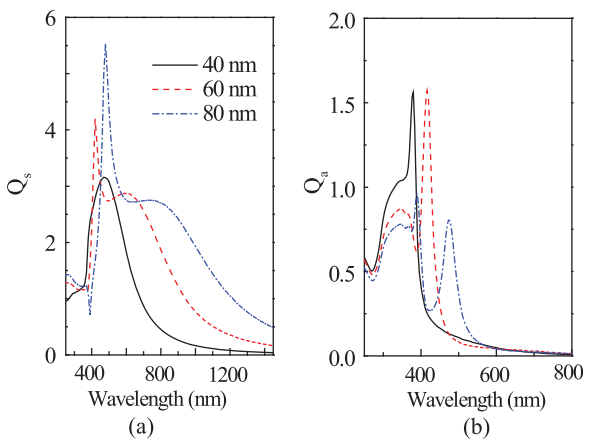

FIG. 4. The angular average (a) scattering and (b) absorption efficiencies an individual NW with different diameters.

B. Reflectance spectra

The measured spectral reflectances of the three NW mats with different average diameters are shown as the solid black curves in Fig. 5. The spectra of all three samples have similar shapes but are also different. All the three samples have relatively small reflectance within the ultraviolet regime (200 to 400 nm), which can be attributed to the relatively weak scattering and strong absorption of silicon NWs. In the visible and near infrared band (from 400 to 1600 nm), the reflectance of all the samples shows a first increase with wavelength to around 50% and then decrease to below 20%. The overall curve shapes are consistent with the results obtained by Street *et al.*[10] For 40, 60, and 80 nm NW mats, the maximum reflection occurs at 556, 646, and 784 nm, respectively. The maximum is located at longer wavelength for the sample with a larger average diameter.

Combining the calculated scattering and absorption efficiencies in Fig. 4 with the two-flux model Eq. (17), it is also possible to calculate the optical reflectance spectra of NWs mats with different diameters, shown as the dashed red curves in Fig. 5. Note that the parameter N_sL in Eq. (17) is quite difficult to obtain from experiments in this case, so it is treated as an unknown parameter and tuned to generate reflectance spectra that match the highest reflectance value of the experimental results. As shown in Fig. 5, an overall agreement with the experiment is seen in both curve shape

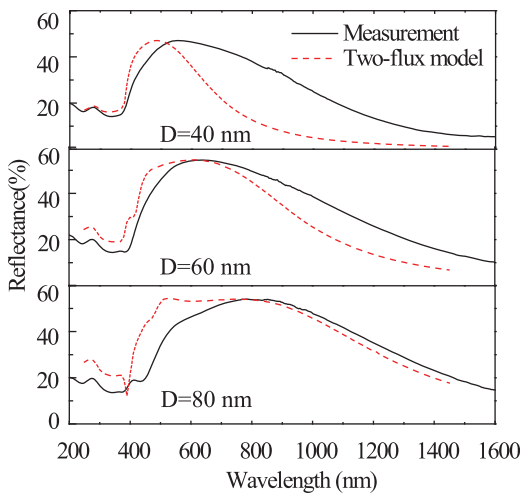

FIG. 5. The total hemispherical reflectance of the random nanowire mats with different diameters: experimental results and the two-flux model.

and reflectance values. The predicted reflectance maxima of the NW mats are located at the similar position as the scattering maxima of the LMR corresponding to $p = 1$, with a little shift towards longer wavelength. For example, for the 40 nm NW sample, the reflectance maximum locates at 490 nm, which is a slightly longer wavelength than the wavelength of the scattering efficiency peak (470 nm). The predicted reflectance maxima do not occur exactly at the wavelength of lowest order LMR scattering peaks because the absorption is larger at this wavelength. Even with the small peak shift, the origin of the reflectance maxima can still be assigned to the lowest order LMR of the individual NWs in the sample. Based on our analysis, the different maxima locations in the two different samples in Ref. 10 can be explained by different NW diameter distributions in the two samples.

Comparing to our measurements, it can be noticed that the predicted reflectance maxima located at slightly shorter wavelengths. The reason for this small shift could be a combination of a few different factors. First, it has been shown that if multiple scattering effect is considered, the scatterer (NWs in this case) could actually have larger effective cross sections than the exact cross section of an individual scatterer.[24–27] Second, we have assumed that the orientations of NWs have equal possibility in any solid angle (Eq. (4)). From Fig. 1, it can be observed that in the samples actually a large number of NWs are in the horizontal direction, especially at the top surface. Those horizontal NWs generally have scattering maxima at a longer wavelength. Therefore, with the assumption that NWs are randomly oriented, we could have underestimated the wavelength where effective reflection maxima occur. There are also noticeable discrepancies the reflectance value for 40 and 60 nm NWs, especially in the long wavelength regime. Note that since N_sL is obtained by matching the peak maximum, the discrepancy when the real N_sL value is used could be smaller in the long wave length regime than it appears in Fig. 5, while the discrepancy around the peak can be larger. It should also be noticed that the discrepancy is larger when the wavelength is longer and NWs are thinner. This could be partly attributed to the multiple scattering effect that is not included in our model.[28] When the wavelength is longer, the interwire distance can be close to or even smaller than the wavelength, so the multiple scattering effects can be more evident[19] and the scattering can be more efficient.[29] The difference between our model and experimental spectra could also be related to the uncertainties in the experiments.

In addition, the volume fraction f of a NW mat is related to N_s by the following equation:

$$f = N_s \pi D^2/4. \tag{18}$$

By assuming the thickness of the NW mats to be 15 μm, the volume fractions of the NW mats can be estimated based on the two-flux model, which is listed in Table I.

Attempts have been made to experimentally obtain the real volume fraction of our samples. However, the weight of the NW mats is too small to be detected by the analytical balance. Based on the SEM images shown in Fig. 1, the volume fractions in Table I should be reasonable.

TABLE I. The volume fractions used in the two-flux model to match the highest reflectance value of the experimental results.

Diameter (nm)	f (%)
40	0.067
60	0.140
80	0.185

C. Further discussion

The reasonable agreement between our predictions and the observed results in the experiment validates our modeling. This indicates that the Mie scattering theory and the two-flux model can be followed to estimate the optical property of random NW mats. It is also possible to extend this method to mats containing different NW diameters by performing further averaging with respect to diameter. To do that, one simply needs to rewrite Eq. (4) into

$$\sigma_i^{avg}(\lambda) = \int_0^\infty \int_0^{\frac{\pi}{2}} \sigma_i(\lambda, D, \theta) f(D) \sin\theta \, d\theta dD, \tag{19}$$

where $f(D)$ is the diameter distribution function of the NWs.

Some limitations of our model have to be pointed out. First, the Mie scattering theory is based on the solution of rigorous Maxwell's equations, so the wave effect is included in the description of each scattering event. But RTE is an equation describing the transport of energy rather than electromagnetic wave, so the wave effect is not considered during the light transport process.[15] It should be noticed that Muskens *et al.* reported strong resonance and enhanced back scattering in GaP NW mats.[30] Those effects cannot be fully captured by the transport theory used here. However, many other NW samples reported in the literature,[9,10,31] including ours, have much smaller volume fractions, so we believe the multiple scattering effect[28] is not important and the transport theory is still applicable. Second, each scattering event at an individual NW is strongly anisotropic. The isotropic assumption is made based on the fact that the NWs are randomly oriented, so the average scattering effect could be close to isotropic. To account for the angular dependence, more complicated radiation models can be applied.[17] However, we believe it is unnecessary here considering all the other uncertainties and approximations.

V. SUMMARY

In summary, the optical reflectances of the silicon NW mats with 40, 60, and 80 nm average diameters are investigated. In the 200 to 400 nm wavelength regime, it is observed experimentally that all silicon NW mats have similar small reflectance, ranging from 15% to 20%. In the 400 to 1600 nm wavelength region, the reflectances of the NW mats are larger. The spectral reflectance of each sample shows a first increase with wavelength to a maximum value and then decrease. Such experimental results can be well reproduced by our analytical model based on Mie scattering theory and two-flux model. This makes it possible to further design the optical properties of NW mats based on physical

quantities, including the dielectric function and the structural parameters of disordered NW mats.

ACKNOWLEDGMENTS

This work is partly supported by the Air Force Office of Scientific Research through the Discovery Challenge Thrust (DCT) Program (Grant No. FA9550-08-1-0126, Program Manager Kumar Jata). HB acknowledges the support of the startup fund from University of Michigan Shanghai Jiaotong University Joint Institute and the Bilsland Dissertation Fellowship from Purdue University. Fruitful discussions with Professor Zhuomin Zhang are also gratefully appreciated.

[1]L. Tsakalakos, J. Balch, J. Fronheiser, B. A. Korevaar, O. Sulima, and J. Rand, Appl. Phys. Lett. **91**, 233117 (2007).
[2]L. Hu and G. Chen, Nano Lett. **7**, 3249 (2007).
[3]O. L. Muskens, J. G. Rivas, R. E. Algra, E. P. A. A. Bakkers, and A. Lagendijk, Nano Lett. **8**, 2638 (2008).
[4]H. Bao and X. L. Ruan, Opt. Lett. **35**, 3378 (2010).
[5]L. Y. Cao, P. Y. Fan, A. P. Vasudev, J. S. White, Z. Yu, W. Cai, J. A. Schuller, S. Fan, and M. L. Brongersma, Nano Lett. **10**, 439 (2010).
[6]L. Cao, P. Fan, E. Barnard, A. Brown, and M. L. Brongersma, Nano Lett. **10**, 2649 (2010).
[7]C. Lin and M. L. Povinelli, Opt. Express **17**, 19371 (2009).
[8]L. Tsakalakos, M. Y. Shih, S. F. LeBoeuf, M. Pietrzykowski, P. J. Codella, B. A. Korevaar, L. V. Sulima, J. Rand, A. Davuluru, and U. Rapol, J. Nanophotonics **1**, 013552 (2007).
[9]A. Convertino, M. Cuscuna, and F. Martelli, Nanotechnology **21**, 355701 (2010).
[10]R. A. Street, W. S. Wong, and C. Paulson, Nano Lett. **9**, 3494 (2009).
[11]G. Brönstrup, F. Garwe, A. Csáki, W. Fritzsche, A. Steinbrück, and S. Christiansen, Phys. Rev. B **84**, 125432 (2011).
[12]Y. Cui, L. J. Lauhon, M. S. Gudiksen, J. Wang, and C. M. Lieber, Appl. Phys. Lett. **78**, 2214 (2001).
[13]H. Bao, X. L. Ruan, and T. S. Fisher, Opt. Express **18**, 6347 (2010).
[14]N. J. Hutchinson, T. Coquil, A. Navid, and L. Pilon, Thin Solid Films **518**, 2141 (2010).
[15]A. Ishimaru, *Wave Propagation and Scattering in Random Media* (Academic, New York, NY, 1978).
[16]Q. Li, B. J. Lee, Z. M. Zhang, and D. W. Allen, J. Biomed. Opt. **13**, 054064 (2008).
[17]S. C. Lee and G. R. Cunnington, Annu. Rev. Heat Transfer **9**, 159–218 (1998).
[18]C. F. Bohren and D. R. Huffman, *Absorption and Scattering of Light by Small Particles* (Wiley, New York, 1983).
[19]M. Kaviany, *Principles of Heat Transfer in Porous Media* (Springer, New York, 1995).
[20]X. L. Ruan and M. Kaviany, Nanoscale Microscale Thermophys. Eng. **9**, 63 (2005).
[21]E. Palik, *Handbook of Optical Constants of Solids* (Elsevier, 1998).
[22]L. Cao, J. Park, P. Fan, B. M. Clemens, and M. L. Brongersma, Nano Lett. **10**, 1229 (2010).
[23]H. C. van de Hulst, Astrophys. J. **112**, 1 (1950).
[24]V. V. Varadan and V. K. Varadan, Phys. Rev. D **21**, 388 (1980).
[25]K. Busch and C. M. Soukoulis, Phys. Rev. Lett. **75**, 3442 (1995).
[26]K. Busch and C. M. Soukoulis, Phys. Rev. B **54**, 893 (1996).
[27]A. Kirchner, K. Busch, and C. M. Soukoulis, Phys. Rev. B **57**, 277 (1998).
[28]C. M. Soukoulis, S. Datta, and E. N. Economou, Phys. Rev. B **49**, 3800 (1994).
[29]S. Redmond, S. Rand, X. Ruan, and M. Kaviany, J. Appl. Phys. **95**, 4069 (2004).
[30]O. L. Muskens, S. L. Diedenhofen, B. C. Kaas, R. E. Algra, E. P. A. M. Bakkers, J. G. Rivas, and A. Lagendijk, Nano Lett. **9**, 930 (2009).
[31]M. A. M. Versteegh, R. E. C. van der Wel, and J. I. Dijkhuis, Appl. Phys. Lett. **100**, 101108 (2012).